Biogeosciences Discuss., 12, 7017–7053, 2015
www.biogeosciences-discuss.net/12/7017/2015/
doi:10.5194/bgd-12-7017-2015

Biogeosciences Discussions
Open Access

Methane distribution, flux, and budget in the East China Sea and Yellow Sea

M.-S. Sun[1,2,*], G.-L. Zhang[1,2], X.-P. Cao[1], X.-Y. Mao[3], J. Li[4], and W.-W. Ye[1]

[1]Key Laboratory of Marine Chemistry Theory and Technology, Ministry of Education, Ocean University of China, Qingdao 266100, China
[2]Qingdao Collaborative Innovation Center of Marine Science and Technology, Ocean University of China, Qingdao 266100, China
[3]College of Physical and Environmental Oceanography, Ocean University of China, Qingdao 266100, China
[4]State Key Laboratory of Satellite Ocean Environment Dynamics, Second Institute of Oceanography, State Oceanic Administration, Hangzhou 310012, China
[*]now at: Helmholtz Center for Ocean Research Kiel (GEOMAR), 24105 Kiel, Germany

Received: 11 March 2015 – Accepted: 23 April 2015 – Published: 12 May 2015

Correspondence to: G.-L. Zhang (guilingzhang@ouc.edu.cn)

Published by Copernicus Publications on behalf of the European Geosciences Union.

Abstract

We measured dissolved methane (CH_4) concentrations, saturations, and fluxes from sea into air and from sediment into water during cruises in March, May, August, October, and December of 2011 in the East China Sea (ECS) and the Yellow Sea (YS). CH_4 concentrations had obvious spatial and seasonal variability due to the complex effects of different water masses and other variables. Maximal CH_4 concentration, sea–air and sediment–water fluxes all occurred during the summer. CH_4 concentration decreased gradually from the coastal area to the open sea, and high levels of CH_4 generally appeared near the Changjiang Estuary and outside the Hangzhou Bay. During early spring and winter, CH_4 had a uniform distribution from the surface to the bottom, but CH_4 concentration increased gradually with depth during other seasons. The subsurface CH_4 maximum occurred at a depth of about 200 m during May, October, and December. The CH_4 level at the bottom was generally higher than at the surface, and this was enhanced during summer due to hypoxia in the bottom waters. Changjiang-diluted water, the Kuroshio Current, and the Taiwan Warm Current Water affected the geographic distribution of CH_4 in the ECS, and these water bodies contributed about 3.45, 2.97, 14.60 mol s^{-1} of CH_4 during summer and 2.11, 8.58, 5.20 mol s^{-1} CH_4 during winter, respectively. Sediment was also a significant source of dissolved CH_4 in the ECS, and we estimated the average sediment–water CH_4 flux of the ECS and YS as about 1.02 µmol m^{-2} d^{-1}. We also used a box model to calculate the CH_4 budget in the ECS. The results suggested that in situ CH_4 production in the water column was the major source of CH_4, and accounted for 0.21 µmol m^{-3} day^{-1} during summer and 0.11 µmol m^{-3} day^{-1} during winter. Air–sea exchange was the major sink of CH_4 in the ECS. We estimated total CH_4 emission from the ECS and YS as about 4.45×10^9 mol during 2011. Our results indicated that the ECS and YS were active areas for CH_4 production and emission.

BGD
12, 7017–7053, 2015

1 Introduction

Methane (CH_4) is an active atmospheric trace gas that is responsible for about 23 % of the global greenhouse effect, and that also participates in atmospheric chemistry and the biogeochemical cycle of global carbon (Crutzen and Zimmermann, 1991; Quay et al., 1999; IPCC, 2013). Atmospheric CH_4 concentration increased at a rate of 12 ± 6 ppb year^{-1} in the 1980s and 6 ± 8 ppb year^{-1} in the 1990s. The global atmospheric CH_4 level was 1773 ± 3 ppb from 1999 to 2006, but the level has increased substantially since 2007, and was reported as 1803 ppb in 2011 (IPCC, 2013). The continuing rise of atmospheric CH_4 indicates an imbalance of sources and sinks. Natural sources are responsible for about 40 % of global CH_4 emission (Shakhova et al., 2010). Among these natural sources, the ocean accounts for only about 0.4–5.0 % of the total (Crutzen, 1991; Bange et al., 1994; Reeburg, 2007).

Microbes oxidize most oceanic CH_4, but this has been mostly ignored, so oceanic CH_4 production might be underestimated (Reeburg, 2007). In marine ecosystems, the variable hydrochemical properties of seawater, especially in shelf and coastal areas, lead to spatial and temporal variations in CH_4 distribution and emission (Zhang et al., 2004, 2008a; Bange, 2004, 2006; Forster et al., 2009). However, oceanic CH_4 emission is poorly quantified, owing to lack of the temporal continuity and areas coverage (Bange et al., 2009). In particular, data on CH_4 in coastal areas of China are scattered and fragmentary (Tsurushima et al., 1996; Zhang et al., 2004, 2008a; Yang et al., 2010). Thus better data on marine CH_4 in coastal seas of China are needed to further optimize the global CH_4 database and completely understand the biogeochemical cycle of CH_4 in the continental shelf area and the regional contribution of this CH_4 to the total global oceanic CH_4 emission.

The East China Sea (ECS) and the Yellow Sea (YS) together forms an important marginal area of the northwestern Pacific Ocean. This is one of the largest continental shelves in the world, with a total surface area of 1.2×10^6 km^2. The ECS opens its north to the YS with the straight line from the northern mouth of the Changjiang

BGD
12, 7017–7053, 2015

(Yangtze River) toward the Jeju Island as the boundary (red dashed line in Fig. 1). The ECS stretches south to the Taiwan Strait, and is adjacent to the western Pacific along its east edge. Its total area is about 7.7×10^5 km^2, and the average water depth is about 72 m. This wide and river-dominated shelf receives large amounts of fresh water (9.03×10^{11} m^3 year^{-1}), sediment (4.14×10^8 t year^{-1}) (Wang et al., 2008), and nutrients (Zhang et al., 1996; Gao et al., 2012) from the Changjiang. The production and transport of particulate matter is related to the redistribution and cycling of bioactive compounds, including dissolved CH_4 (Karl and Tilbrook, 1994). Coastal currents along mainland China, the Taiwan Warm Current, and a branch of the Kuroshio Current, which has significantly different effects in dry seasons and in flood seasons (dominated by monsoons and Changjiang runoff) (Su, 1998; Zhang et al., 2007), drive circulation in the ECS. Researchers have recently focused on this area due to its unique geography and the beneficial effects of its biogeochemical cycles of nutrients and organic matter.

In this paper, we characterize the spatial distribution and seasonal variation of dissolved CH_4 in the ECS and YS (Fig. 1) based on data collected during five cruises in 2011, and identify factors that affected these patterns. We also estimate fluxes at the sea–air and sediment–water interfaces to determine the amount of CH_4 released by the ECS into the atmosphere and the amount that escaping from sediments into the ECS. We use a box model to calculate the CH_4 budget in the ECS, identify the main sources and sinks of dissolved CH_4 in this area, and estimate the contribution of different sources to total CH_4 quantitatively. We also provide a rough estimate of CH_4 production in the continental shelf area based on calculations of water mass mixing. The ultimate aims of this research are to provide a more thorough understanding of dissolved CH_4 in the ECS, improve knowledge of global marine CH_4, and identify a method for calculation of oceanic CH_4 production rate based on results from physical ocean surveys.

BGD
12, 7017–7053, 2015

2 Materials and methods

2.1 Seawater sampling and analysis

Five cruises were conducted in the ECS and YS during 2011 for collection of data at different locations (Fig. 1, Table 1). Seawater samples were collected at different depths using 5 or 8 L Niskin bottles mounted to a Sea-Bird CTD rosette. Surface waters were collected at a depth of ~ 2 m, and bottom waters were typically collected at ~ 3 m above the seafloor. Two subsamples for CH_4 determinations were transferred from the Niskin bottles into glass vials (~ 117 mL) using a silicone tube. After overflow of approximately 1.5- to 2-fold of bottle volume, 1 mL of a saturated solution of $HgCl_2$ was added to inhibit microbial activity. Then, the sample bottle was immediately sealed with a butyl rubber stopper and an aluminum cap (to exclude excess water) and stored upside down in a dark box (Zhang et al., 2008a). All water samples were analyzed after return to the laboratory, within 60 days after collection (Zhang et al., 2004). Salinity and temperature data were also measured by the CTD, and wind speeds were measured by the shipboard automatic weather stations at about 10 m above the sea surface.

Dissolved CH_4 from seawater samples was measured using a gas-stripping method and a GC-14B gas chromatograph (Shimadzu, Japan) with a flame ionization detector (FID) (Zhang et al., 2004). FID responses were calibrated using known volumes of CH_4 standards (2., 4., and 50.0 ppmv, Research Institute of China National Standard Materials). There was a linear relationship between FID response and CH_4 concentration, so a multi-point calibration method was used to determine CH_4 concentration based on chromatographic peak area. This method had a precision better than 3 % (Zhang et al., 2004).

2.2 Sediment sampling and incubation experiments

The emission of CH_4 from sediments was measured by the closed chamber incubation method (Barnes and Owens, 1999). Sediment samples were collected by a box corer

BGD
12, 7017–7053, 2015

at different sampling stations (Fig. 1, red triangles). Only samples with undisturbed sediment surfaces were used. At each station, 15 sediment cores were collected using plexiglass tubes that had openings on both ends (i.d. = 5 cm, height = 30 cm), with the bottoms sealed using air-tight rubber bungs. Just prior to the beginning of flux measurements, ambient bottom water was added carefully (with no gas headspace), and then the core was capped with a Plexiglass top that had gas-tight O-ring seals and two sampling ports. All cores were arranged around a central shaft which was supported by magnets that rotated at 60 rpm, and were placed in a water-filled tank that was held at ambient temperature using a recirculating water temperature-controlled bath. Ten glass bottles filled with ambient bottom water were placed in the same tank and used as a water column control. Cores were incubated in the dark for 24 ~ 48 h. Three overlying water samples were collected at 4 to 8 h intervals, transferred into 56.5 mL glass bottles, and treated with 0.5 mL $HgCl_2$ to inhibit microbial activity. At the same time, two bottled water samples were also treated with 0.5 mL $HgCl_2$ as a water column control. The CH_4 concentrations of all samples were measured by the gas-stripping method described above. Sediment–water CH_4 flux was estimated from the slope of the CH_4 increase in the overlying water as a function of time. The discrepancy in the rate of sediment CH_4 emission that resulted from differences between incubation temperatures and the in situ temperatures was calibrated by the Arrhenius empirical equation.

2.3 Saturation and sea-to-air flux calculations

The saturation (R, %) and sea-to-air flux (F, $\mu mol\,m^{-2}\,d^{-1}$) of CH_4 were calculated by the following formulas:

$$R\ (\%) = C_{obs}/C_{eq} \times 100 \quad (1)$$

$$F = k \times (C_{obs} - C_{eq}) \quad (2)$$

where C_{obs} is the observed concentration of dissolved CH_4 and C_{eq} is the air-equilibrated seawater CH_4 concentration, calculated from the in situ temperature and

BGD
12, 7017–7053, 2015

salinity and the solubility data of Wiesenburg and Guinasso (1979). Atmospheric CH_4 was not measured in this study. Instead, a mean atmospheric CH_4 mixing ratio of 1902 ppb at three observation stations near the East China Sea (LLN, TAP and SDZ) in 2011, from the NOAA/ESRL Global Monitoring Division in situ program (http://www.esrl.noaa.gov/gmd), was used for all calculations. In formula 2, k stands for the gas transfer coefficient, which is a function of wind speed and Schmidt number (Sc), generally estimated by the empirical equations. Various empirical equations were published to estimate k. Nightingale et al. (2000) reported an evaluation of sea–air gas exchange in coastal ocean, and the corresponding value lies near the median of extensive methods and models (Cockenpot et al., 2015). Wanninkhof (2014) improved the methodology and updated the relationship between gas exchange and wind speed based on his previous research over the last two decades (Wanninkhof, 1992). These two methods (hereafter N2000 and W2014) were chosen to calculate air–sea fluxes since they are more representative and trustworthy.

3 Results

3.1 Hydrography of the ECS

The hydrography of the ECS is variable due to succession of the Kuroshio Current and the low-salinity coastal water. Three main water masses influence the ECS throughout the year: Changjiang-diluted water, Taiwan Warm Current Water, and Kuroshio Current (Su, 1998; Li and Su, 2000; Zhang et al., 2007; Qi et al., 2014). These effects are evident in the temperature–salinity (T–S) curves along all sections during May, October, and December (Fig. 2). The salinities at stations near the Changjiang Estuary (i.e. C0, B1 in May; P01, F03 in October; F02, P01 in December) were less than 32 practical salinity units (psu), due to the effect of Changjiang Diluted Water (CDW). In contrast, the Kuroshio Current affected the T–S relationships at stations on the continental slope (i.e. CJ, D1, D9, ED and G8 in May; P12, E10 in October; E10 in December). Moreover,

BGD
12, 7017–7053, 2015

water columns of these stations could be divided into four layers according to their T–S relationships: (i) Kuroshio surface water (KSW) was present at a depth of 0 ~ 50 m, and this water had high temperature and salinity; (ii) Kuroshio subsurface water (KSSW) was at a depth of 50 ~ 300 m, and this water had a lower temperature than the surface water; (iii) Kuroshio intermediate water (KIW) was present at a depth of 300 ~ 800 m, and had lower salinity and temperature than the upper water; and (iv) Kuroshio deep water (KDW) was at 800 m and lower, and this high-density water had a temperature of about 5 °C.

The Taiwan Warm Current Water (TWCW) also affected the mid-shelf of the ECS, as indicated by the high temperature and a moderate salinity 33.0 ~ 34.5 psu in the southwestern region of the ECS (stations T01, T03 in May; Z01, Z03 in October; Z02, Z03 in December). The shelf water mixed with water from the CDW, TWCW, KSW, and KSSW, and its salinity was 32 ~ 34 psu. High CH_4 levels were usually present in areas impacted by the CDW, and low CH_4 levels were present in the water from the Kuroshio Current. The intermediate level of CH_4 in the broad shelf suggested a mixing of these two water masses.

3.2 Seasonal variations of CH_4 in the ECS and YS

Table 2 shows the temperature, salinity, and CH_4 concentrations in surface and bottom waters of the ECS and YS during the five cruises of 2011. CH_4 concentration had an obvious seasonal variation, with the highest level in summer and the lowest level in winter and early spring (March). CH_4 concentrations in late spring (May) were comparable to those in autumn and about 40 % lower than those in summer. The salinity during August was the lowest due to the surge of Changjiang runoff in summer. CH_4 concentration in the Changjiang River (135.3 ± 36.9 nmol L^{-1}) was about 10–30 times higher than in the ECS (Zhang et al., unpublished data), and this increased CH_4 concentration in the whole ECS. During the five cruises, bottom-level CH_4 concentrations were all higher than those at the surface, especially during summer when bottom-level CH_4 was 11.88 ± 4.59 nmol L^{-1}, about 2 ~ 4-fold higher than during other seasons.

BGD
12, 7017–7053, 2015

3.3 Geographic Distribution of CH_4 in the YS and ECS

Figure 3 shows the geographic distributions of temperature, salinity, and CH_4 in surface and bottom waters of the YS and ECS in 2011. Two cruises were in spring (March, Fig. 3a; May, Fig. 3b). During May, surface and bottom water temperature increased gradually from north to south, and temperature was relatively low ($2 \sim 3\,^{\circ}C$) in the bottom water on the edge of the ECS continental shelf. Surface and bottom salinity increased gradually from the Changjiang Estuary to the southeast. Dissolved CH_4 concentrations in surface and bottom waters gradually declined from the Changjiang Estuary towards the open sea during spring. High CH_4 concentrations in the surface water appeared near Changjiang Estuary (T05: 29.67 nmol L^{-1} in March; C0: 21.38 nmol L^{-1} in May) due to the Changjiang-diluted water. CH_4 concentrations in the bottom were slightly higher than in the surface, and high levels at F03 (30.63 nmol L^{-1}) and F04 (19.58 nmol L^{-1}) during March and at B1 (17.81 nmol L^{-1}) and D1 (20.01 nmol L^{-1}) during May. In the southeastern continental shelf of the ECS, CH_4 concentrations were relatively low (about $2 \sim 3$ nmol L^{-1}), mainly due to the influence of the CH_4-depleted Kuroshio surface water.

Temperature in the surface and bottom waters increased from north to south during August (Fig. 3c). Salinity had a similar trend during spring, but Changjiang-diluted water had an obvious extension in the ECS during summer, and surface salinity was below 32 psu at most regions of the continental shelf in the ECS. Dissolved CH_4 increased with temperature and freshwater discharge during summer (about 33 484 $m^3\,s^{-1}$, more than 2 times than during spring; Changjiang Water Resources Committee, 2011). The mean surface and bottom CH_4 concentrations were 8.21 ± 6.02 nmol L^{-1} and 11.88 ± 4.59 nmol L^{-1}, respectively. Just as in spring, high CH_4 concentrations in the surface and bottom waters were present near the Changjiang Estuary and outside Hangzhou Bay. Particularly, bottom CH_4 concentrations were high ($10.51 \sim 12.48$ nmol L^{-1}) in the high turbidity zone of the Changjiang Estuary ($\sim 122^{\circ}00'$–$122^{\circ}20'$ E, $30^{\circ}50'$–$31^{\circ}15'$ N; Shen, 2012), and this corresponded to low oxygen concentrations ($2.10 \sim 2.82$ mg L^{-1})

BGD
12, 7017–7053, 2015

in this area. Besides, high temperature during summer may lead to water stratification, which prevents dissolved CH_4 in bottom waters from diffusing into upper waters, and thereby further increased the CH_4 level in the bottom water.

During the October survey, surface seawater temperature and salinity increased gradually from northwest to southeast (Fig. 3d). Bottom temperatures in the ECS were almost all in the range of 19 ~ 22 °C, but there was a cold bottom center (below 10 °C) on the southeastern region of the YS. Water with high temperature and salinity at the southeastern corner of the survey area might have been affected by the northward branch of the Kuroshio Current. CH_4 concentrations during autumn were significantly lower than during summer. Bottom CH_4 concentrations of the entire ECS shelf were relatively high (above 8.0 nmol L^{-1}), especially at coastal areas, i.e. the Changjiang Estuary (P01, P03), the mouth of Hangzhou Bay (T05), and the surrounding waters of Jeju Island (A10, D07). On the contrary, CH_4 concentrations were quite low (about 3 nmol L^{-1}) in the southeastern part of the ECS continental shelf, and this can also be attributed to the CH_4-depleted Kuroshio Current.

The geographic distributions of surface and bottom temperature and salinity during December (Fig. 3e) were similar to that recorded during October, but Changjiang-diluted water had a slight influence. The CH_4 level of the whole ECS and YS during December was far below the levels during August and October, and the average CH_4 concentration in the surface waters (4.07 nmol L^{-1}) was slightly lower than that in the bottom waters (4.53 nmol L^{-1}). Surface CH_4 concentrations in the YS were slightly higher than those in the ECS, and high CH_4 concentrations occurred in the southern YS near Cheju Island, while sporadically high levels of CH_4 in the bottom waters mainly occurred near the continental slope in the ECS. To sum up, CH_4 concentrations in the surface and bottom waters of the YS and ECS during winter were uniform and stable, and were 3 ~ 5 nmol L^{-1} in most regions.

BGD
12, 7017–7053, 2015

3.4 Depth distribution of CH_4 in the ECS

Section PN (red solid line in Fig. 1) extends from the Changjiang Estuary southeast towards the Okinawa Trough and across the Changjiang-diluted water and the mainstream of the Kuroshio. Section E (purple solid line in Fig. 1) also lies across the entire shelf of the ECS, and extends from the coastal area of Zhejiang and Fujian provinces east towards the Okinawa Trough. We used these representative sections to study the hydrological and chemical characteristics of the ECS. Here we choose the top buoyant water (depth less than 200 m) to analyze the depth distribution of dissolved CH_4 on the ECS shelf.

Figure 4 shows the depth distributions of temperature, salinity, and CH_4 along section P during March and October, section CJ during May, and section E during December. Seawater temperature and salinity gradually increased with distance from the shore, but the depth profiles had seasonal variations. During early spring (March, Fig. 4a) and winter (December, Fig. 4d), the water column was well-mixed in the top 100 m, and temperature and salinity along section P were uniform from the surface to the bottom; however, the depth profiles of temperature and salinity were stratified during late spring (May, Fig. 4b) and autumn (October, Fig. 4c). The water column in the middle shelf of the ECS became stratified during late spring, but this stratification faded during the fall and disappeared completely during December.

Correspondingly, dissolved CH_4 concentrations along section PN and section E gradually decreased with distance from the shore, and the maximum CH_4 concentration of surface water was near the shore. During March and December, CH_4 concentrations were relatively uniform from surface to bottom, but CH_4 concentrations increased gradually with depth during May and October. Particularly, high bottom CH_4 values were usually present at stations close to the continental shelf, especially the shelf break area. Surprisingly, the bottom CH_4 concentration at P09 during October reached 12.16 nmol L^{-1}, almost 2-fold greater than the surface level.

BGD
12, 7017–7053, 2015

Figure 5 shows depth profiles of seawater temperature, salinity, and CH_4 concentrations at CJ, P12, and E10 at depths of 2 to 1000 m. Seawater temperature decreased gradually with depth, and there was a sharp decline at about 75 m. However, salinity increased at first and then declined sharply at about 150 m, with a slight increase below 500 m. All CH_4 concentrations increased initially with depth, and then decreased to 500 m, and maximum CH_4 levels occurred at 200 m during May, October, and December. Previous research documented a subsurface CH_4 maximum at the base of the mixed layer (about 40–150 m), which occasionally coincided with the pycnocline (Brooks et al., 1981; Burke et al., 1983; Oudot et al., 2002). Remarkably, there were two peaks in the CH_4 depth profiles during spring and autumn, and the second peak occurred at a depth of 600 m during May and at 800 m during October. CH_4 concentrations further increased below 800 m, and there were high CH_4 levels in the bottom waters during May and December.

3.5 Sediment–water CH_4 fluxes in the YS and ECS

Sediment–seawater fluxes of CH_4 from the ECS and YS had an obvious seasonal variation, with maxima during summer (Fig. 6) when the flux was about 2 times higher than the other seasons. CH_4 was emitted from the sediments at most stations and acted as a net source of CH_4 in the water column. CH_4 release from sediments also had obvious spatial and temporal variation. The bottom water incubation experiments ("sample" in Fig. S1 in the Supplement) at P01 indicated that the CH_4 concentration in the overlying waters increased linearly with incubation time (t) (March: $[CH_4] = 0.59 \times t + 6.33$, $r^2 = 0.73$; October: $[CH_4] = 0.19 \times t + 2.64$, $r^2 = 0.85$; December: $[CH_4] = 0.23 \times t + 4.37$, $r^2 = 0.95$), and the sediment–seawater CH_4 flux at P01 was 1.93 $\mu mol\,m^{-2}\,d^{-1}$ during March, 0.72 $\mu mol\,m^{-2}\,d^{-1}$ during October and 1.60 $\mu mol\,m^{-2}\,d^{-1}$ during December, respectively. Station C1 (near the Changjiang river mouth) had a sediment–water CH_4 flux of 2.94 $\mu mol\,m^{-2}\,d^{-1}$ during August, much higher than any other sites; this might be ascribed to the low oxygen concentration in

BGD
12, 7017–7053, 2015

the overlying water (3.25 mg L^{-1} based on Winkler titration) and the rich organic carbon in the sediment (Lin et al., 2002; Kao et al., 2003). Average sediment–water CH_4 flux of the ECS and YS was about 1.02 µmol m^{-2} d^{-1} in 2011. Based on their total surface areas (about 1.15×10^6 km^2), the annual CH_4 emission from sediments of the ECS and YS in 2011 was about 4.28×10^8 mol. This indicated that sediments were an important source of CH_4 in the bottom waters. However, the estimate of CH_4 released from sediment had limited certainty because of the scant sampling stations in each survey and the high spatial variation of sediment–water CH_4 flux.

3.6 Sea–air CH_4 fluxes in the YS and ECS

Table 3 shows surface CH_4 saturations and sea–air CH_4 fluxes in ECS and YS. Dissolved CH_4 saturations varied significantly among the seasons, and the maximum CH_4 saturation was during summer, followed by spring, autumn, and winter. Yang et al. (2010) reported that average surface CH_4 saturation in the YS was highest (515.2 ± 231.5 %) during August 2006, in agreement with our results. Riverine water is often oversaturated with CH_4 (Zhang et al., 2008b; Middelburg et al., 2002; Upstill-Goddard et al., 2000); in agreement, we found higher CH_4 saturation near the Changjiang Estuary and outside Hangzhou Bay. We recorded the highest CH_4 saturation at station T05 (1007 %) in March, station C0 (858 %) in May, and station E01 (1558 %) in August. In general, the surface waters of the YS and ECS were all oversaturated with CH_4, except for a few stations during spring. Thus, the YS and the ECS were net sources of atmospheric CH_4.

Sea–air CH_4 fluxes calculated with the N2000 equation were approximate to the results from the W2014 equation, and they also had seasonal variations, with the greatest flux during summer. In August, sea–air flux of the Changjiang Estuary and its adjacent sea area was about 9.9 µmol m^{-2} d^{-1}, while Zhang et al. (2008a) reported that sea–air CH_4 flux in the shelf-mixed water of the ECS was merely 2.81–6.89 µmol m^{-2} d^{-1} during summer. This indicated that coastal sea–air exchange of CH_4 was extremely intense,

BGD
12, 7017–7053, 2015

much greater than on the shelf area. According to W2014 equation, the annual average sea–air CH_4 flux from the ECS and YS was about 10.59 µmol m^{-2} d^{-1} during 2011. Based on the areas of the YS (~ 380 000 km^2) and ECS (~ 770 000 km^2), we estimated total CH_4 emission from the ECS and YS as 4.45×10^9 mol (about 0.71 Tg) during 2011. Bange (1994) estimated the global oceanic CH_4 emission was 11–18 Tg CH_4 $year^{-1}$, so the YS and ECS accounted for about 0.49 % of the global total. This value was much higher than its corresponding area proportion of 0.32 %, indicating that the YS and ECS were active areas for CH_4 production and emission.

4 Discussion

4.1 Factors influencing CH_4 distribution in the ECS and YS

The concentration, saturation, and sea–air and sediment–water fluxes of CH_4 in the ECS and YS all had obvious seasonal variations. Mean CH_4 saturation (R_{CH_4}) had a linear correlation with mean water temperature (T) in the surface water ($R_{CH_4} = 13.91 \times T - 3.10$, $r^2 = 0.77$; Fig. S2) and bottom water ($R_{CH_4} = 33.50 \times T - 225.03$, $r^2 = 0.76$; Fig. S2) during different seasons. Temperature can also increase the production of CH_4 in sediments, and CH_4 production rate increases with temperature in the range of 0–30 °C (Liikanen et al., 2002; Glissmann et al., 2004). Besides, the rising temperature may increase the relative abundance and diversity of methanogenic communities (Høj et al., 2008; Metje and Frenzel, 2005). Yvon-Durocher et al. (2014) reported seasonal variations of CH_4 emissions from diverse ecosystems using meta-analysis, and showed that CH_4 emissions increased significantly with seasonal increases of temperature; this seasonal increase in CH_4 production derived from methanogens and anaerobic microbial communities. Our results were consistent with these previous studies, and supported the view that water temperature played a significant role in regulating the seasonal variation and distribution of CH_4 in the ECS and YS.

BGD
12, 7017–7053, 2015

CH_4 formation and consumption in the water column are also important factors that influence the distribution of CH_4 in the ECS and YS. Subsurface methane maxima were observed in this study, which has been considered to be a common phenomenon in the open sea (Reeburgh, 2007). Early studies demonstrated that advective transport of CH_4 or in situ CH_4 production by microbes in hypoxic microenvironments led to excess CH_4 in the mixed layer (Scanton and Brewer, 1977; Angelis and Lee, 1994). More recent results suggested that in nutrient-limited conditions, a variety of methyl-rich organic phosphorus or sulfur compounds were all likely to be utilized by microorganism and served as precursors of CH_4 production (Karl et al., 2008; Damm et al., 2008; Zindler et al., 2013; Lennin et al., 2013). The bottom water incubation experiments ("water column control" in Sect. 2.2; "blank" in Fig. S1) at some stations (L1 in May, J1 in August, A10 and A02 in October and R07 in December) indicated that the CH_4 concentration in the bottom waters increased linearly with incubation time. This suggested that in situ CH_4 production might be another source of the excess CH_4 in the bottom waters. Moreover, CH_4 is more likely to be produced in anoxic environments that have sufficient organic carbon (Jayakumar et al., 2001; Naqvi et al., 2010; Bange et al., 2010). The low oxygen level (2.00–4.00 $mg\,L^{-1}$) and high particulate organic carbon flux (3900–7300 $mg\,C\,m^{-2}\,d^{-1}$; Hung et al., 2013) near the Changjiang Estuary and outside Hangzhou Bay favored CH_4 production in the bottom waters of these areas.

The CH_4 concentration of the Changjiang water was about 10–40 times higher than that of the ECS, and the discharge of freshwater from the Changjiang into the ECS was much greater during summer than winter (Table 4), therefore the widespread dispersal of Changjiang plume had a greater impact on CH_4 distribution than that in winter. Similar to the CDW, the Kuroshio and TWCW had different effects on the ECS during summer and winter. During summer, water input from the TWCW ($2.39 \times 10^6\ m^3\,s^{-1}$) was much greater than that from the Kuroshio ($0.89 \times 10^6\ m^3\,s^{-1}$) (Zhang et al., 2007), and the CH_4 level of the TWCW (6.11 $mol\,L^{-1}$, Ye et al., 2015) was almost two-fold greater than that of the Kuroshio (2.91 $mol\,L^{-1}$). Thus, during summer, the TWCW had a larger influence on distribution of CH_4 in the ECS than the Kuroshio; during winter,

BGD
12, 7017–7053, 2015

they had comparable contributions due to their more similar water discharges and CH_4 concentrations. Thus, the mixing of different water masses and their seasonal variations directly impact CH_4 distribution of the ECS.

4.2 Preliminary estimate of CH_4 budget in the ECS

In order to quantify the contributions of different sources and sinks to dissolved CH_4 in the ECS, CH_4 budget was estimated based on data presented here and previous research. Zhang et al. (2007) re-estimated the nutrient budget of the ECS using a box model during summer and winter. According to mass conservation, the water and salinity balance of the ECS can be expressed as:

$$\sum_{i=1}^{n} \mathrm{WFi} + \Delta Q = 0 \quad (3)$$

$$\sum_{i=1}^{n} \mathrm{WFi} \times \mathrm{Ci} + \Delta \mathrm{Mi} = 0 \quad (4)$$

where WFi represents the water flux of inputs (+) and outflows (−) over the shelf; ΔQ is the water mass distinction caused by sea level change in the ECS; Ci is the salinity or value of a certain element for a known water mass; and ΔMi is the increase or decrease of the given element during exchange at the sediment–water and sea–air interface. The inflow to the ECS Shelf includes water from the Taiwan Strait (TWCW), riverine input from the land-mass (of which the Changjiang accounts for about 90–95 % or more), and incursion of the Kuroshio from north of Taiwan and over the broad shelf mainly composed of KSW (~ 25 %) and KSSW (~ 75 %) (Zhang et al., 2007). The exchange between the ECS and the YS is taken into account as well. The outflow refers to currents through the Tsushima/Korea Strait (Zhang et al., 2007). We did not consider groundwater, because only limited data were currently available for the ECS.

As with the shelf water budget in the ECS (Zhang et al., 2007), we estimated the budget of dissolved CH_4 for summer and winter. The Kuroshio and TWCW were hardly

BGD
12, 7017–7053, 2015

observed during our summer cruise because of the limited investigation region, so the corresponding data were from the literature (Ye et al., 2015) and unpublished data of the ECS that was collected during July 2013. Data for riverine CH_4 were from our on-going monitoring project at station in Xuliujing, at the lower Changjiang. Considering that the sea–air fluxes values from W2014 and N2000 were quite similar, we took W2014 for budget calculation. Table 4 lists the discharges of various water masses and their CH_4 concentrations, and Fig. 7 shows a preliminary estimate of the CH_4 budget in the ECS. We ignored the effects of evaporation and precipitation because of unavailable data and the low water fluxes of these processes. During summer, the TWCW transported 14.60 mol s^{-1} of CH_4, the Kuroshio transported 2.97 mol s^{-1} of CH_4, the CDW transported 3.45 mol s^{-1} of CH_4, and sediment released 15.86 mol s^{-1} of CH_4. However, CH_4 emission at the sea–air interface reached 151.33 mol s^{-1} and CH_4 export from the ECS was 18.12 mol s^{-1}. Thus, to maintain a balance of the CH_4 in the ECS, the in situ net CH_4 formation rate should be 132.51 mol s^{-1}.

During winter, the Kuroshio imported 5.28 mol s^{-1} of CH_4 into the ECS (1.8-fold more than in summer), and the TWCW imported 5.20 mol s^{-1} of CH_4 (1/3 of that in summer). Although the winter discharge of the Changjiang was almost equal with that of the YS, CH_4 input by Changjiang (2.11 mol s^{-1}) was significantly higher than that from the YS (0.06 mol s^{-1}). CH_4 emission from sediments was 8.38 mol s^{-1} during winter, and CH_4 release from the ECS into the atmosphere was about 81.01 mol s^{-1}. Thus, the average net CH_4 production rate of seawater during winter must be 73.12 mol s^{-1} to balance the CH_4 loss by sea–air exchange and outflow. The results above suggested that in situ CH_4 production in the water column was the major source of CH_4 in the ECS, accounting for more than 70 % of CH_4 input from all sources, and that the main external sink was sea–air exchange, accounting for about 90 % of CH_4 export.

Considering the area and average depth of the ECS, we estimated the mean net CH_4 production rate of seawater in the water column as 0.21 µmol m^{-3} d^{-1} during summer and 0.11 µmol m^{-3} d^{-1} during winter. However, del Valle and Karl (2014) calculated the

BGD
12, 7017–7053, 2015

CH_4 budget in the mixed layer at station ALOHA (in the open sea, north of Hawaii) and estimated the net CH_4 production rate in the mixed layer ranged from 0.008–0.047 $\mu mol\,m^{-3}\,d^{-1}$ from September 2012 to September 2013, much lower than our estimate. Thus, it can be inferred that CH_4 production in the water column of the ECS was much more powerful than in the open sea, and the rate of CH_4 production may be higher in bottom water than in surface water.

However, these results have large uncertainties, due to potential errors in the deviation of method and in calculations of sea–air and sediment–water fluxes. Due to the limitations of available data, we did not consider CH_4 input from groundwater into the ECS. We performed sediment incubations at several stations, but the results cannot be considered representative of sediment emission from the whole ECS. Although our method of estimation was not perfect, no direct measurements were yet available for determination of in situ CH_4 production in the ECS. Here we provided a rough value of CH_4 production in the continental shelf that were calculated by water mass mixing, and offered new insights into CH_4 production in the ocean.

5 Conclusions

The distribution and emission of CH_4 had obvious seasonal variations in the ECS and YS, and there were also regional differences due to various factors, including differences in the mixing of water masses, water temperature, freshwater input, sediment release, and oxygen levels in the water column. We estimated the CH_4 budget of the ECS using a box model, and the results indicated that sediments (15.86 $mol\,s^{-1}$) and the Taiwan Warm Current Water (14.60 $mol\,s^{-1}$) were the main external sources of CH_4 during summer. During winter the total CH_4 inputs from the various sources were lower, but sediment remained as the largest external source (8.38 $mol\,s^{-1}$). The Changjiang diluted water had a significant impact on CH_4 during summer (3.45 $mol\,s^{-1}$) and winter (2.11 $mol\,s^{-1}$). The most important source of CH_4 in the ECS was in situ production in

BGD
12, 7017–7053, 2015

the water column, which accounted for more than 70 % of the CH_4 in the ECS. Sea–air exchange was the major external sink of CH_4 in the ECS, and we estimated that the ECS and the YS released about 4.45×10^9 mol of CH_4 $year^{-1}$ into the atmosphere.

The Supplement related to this article is available online at doi:10.5194/bgd-12-7017-2015-supplement.

Author contributions. M.-S. Sun collected and analyzed water samples in October and December 2011. G.-L. Zhang designed the sampling strategy. M.-S. Sun and G.-L. Zhang prepared the manuscript. X.-P. Cao collected and analyzed water samples in March, May, and August 2011. X.-Y. Mao provided hydrological data for March, October and December of 2011. J. Li provided hydrological data for May and August of 2011. W.-W. Ye provided some data for calculation of the methane budget of the East China Sea.

Acknowledgements. The authors wish to thank the crews of the R/V "*Dong Fang Hong 2*", the R/V "*BeiDou*" and the R/V "*Experiment 3*" and colleagues from the Laboratory of Marine Biogeochemistry, Ocean University of China for assistance in collection of field samples. This study was funded by the Ministry of Science and Technology of China through Grant no. 2011CB409802, 2010CB428904 and 2011CB409803 supported by the National Science Foundation of China through Grant no. 41221004, and by the 111 Project (B13030). This is MCTL Contribution no. 76. M.-S. Sun is especially grateful for the scholarship provided by the China Scholarship Council during her study in Germany.

References

Bange, H. W.: Air–sea exchange of nitrous oxide and methane in the Arabian Sea: a simple model of the seasonal variability, Indian J. Mar. Sci., 33, 77–83, 2004.

Bange, H. W.: Nitrous oxide and methane in European coastal waters, Estuarine, Estuar. Coast. Shelf S., 70, 361–374, doi:10.1016/j.ecss.2006.05.042, 2006.

BGD
12, 7017–7053, 2015

Bange, H. W., Bartell, U. H., Rapsomanikis, S., and Andreae, M. O.: Methane in the Baltic and North Seas and a reassessment of the marine emissions of methane, Global Biogeochem. Cy., 8, 465–480, doi:10.1029/94GB02181, 1994.

Bange, H. W., Bell, T. G., Cornejo, M., Freing, A., Uher, G., Upstill-Goddard, R. C., and Zhang, G. L.: MEMENTO: a proposal to develop a database of marine nitrous oxide and methane measurements, Environ. Chem., 6, 195–197, 2009.

Bange, H. W., Bergmann, K., Hansen, H. P., Kock, A., Koppe, R., Malien, F., and Ostrau, C.: Dissolved methane during hypoxic events at the Boknis Eck time series station (Eckernförde Bay, SW Baltic Sea), Biogeosciences, 7, 1279–1284, doi:10.5194/bg-7-1279-2010, 2010.

Barnes, J. and Owens, N. J. P.: Denitrification and nitrous oxide concentrations in the Humber estuary, UK, and adjacent coastal zones, Mar. Pollut. Bull., 37, 247–260, doi:10.1016/S0025-326X(99)00079-X, 1999.

Brooks, J. M., Reid, D. F., and Bernard, B. B.: Methane in the upper water column of the northwestern Gulf of Mexico, J. Geophys. Res.-Oceans, 86, 11029–11040, doi:10.1029/JC086iC11p11029, 1981.

Burke Jr., R. A., Reid, D. F., Brooks, J. M., and Lavoie, D. M.: Upper water column methane geochemistry in the eastern tropical North Pacific, Limnol. Oceanogr., 28, 19–32, 1983.

Changjiang Water Resources Committee: Changjiang Sediment Bulletin, P. R. C. Minister of Water Resources, Changjiang Press, Wuhan, China, 43 pp., 2011 (in Chinese).

Cockenpot, S., Claude, C., and Radakovitch, O.: Estimation of airewater gas exchange coefficient in a shallow lagoon based on ^{222}Rn mass balance, J. Environ. Radioactiv., 143, 58–69, doi:10.1016/j.jenvrad.2015.02.007, 2015.

Crutzen, P. J. and Zimmermann, P. H.: The changing photochemistry of the troposphere, Tellus B, 43, 136–151, 1991.

Damm, E., Kiene, R. P., Schwarz, J., Falck, E., and Dieckmann, G.: Methane cycling in Arctic shelf water and its relationship with phytoplankton biomass and DMSP, Mar. Chem., 109, 45–59, doi:10.1016/j.marchem.2007.12.003, 2008.

De Angelis, M. A. and Lee, C.: Methane production during zooplankton grazing on marine phytoplankton, Limnol. Oceanogr., 39, 1298–1308, 1994.

Del Valle, D. A. and Karl, D. M.: Aerobic production of methane from dissolved water-column methylphosphonate and sinking particles in the North Pacific Subtropical Gyre, Aquat. Microb. Ecol., 73, 93–105, doi:10.3354/ame01714, 2014.

BGD
12, 7017–7053, 2015

ESRL's Global Monitoring Division: available at: http://www.esrl.noaa.gov/gmd (last access: 6 April 2015), 2015.
Florez-Leiva, L., Damm, E., and Farías, L.: Methane production induced by dimethylsulfide in surface water of an upwelling ecosystem, Prog. Oceanogr., 112, 38–48, doi:10.1016/j.pocean.2013.03.005, 2013.
Forster, G., Upstill-Goddard, R. C., Gist, N., Robinson, C., Uher, G., and Woodward, E. M. S.: Nitrous oxide and methane in the Atlantic Ocean between 50° N and 52° S: latitudinal distribution and sea-to-air flux, Deep-Sea Res. Pt. II, 56, 964–976, doi:10.1016/j.dsr2.2008.12.002, 2009.
Gao, L., Li, D., and Zhang, Y.: Nutrients and particulate organic matter discharged by the Changjiang (Yangtze River): seasonal variations and temporal trends, J. Geophys. Res.-Biogeo., 117, 1–16, doi:10.1029/2012JG001952, 2012.
Glissman, K., Chin, K. J., Casper, P., and Conrad, R.: Methanogenic pathway and archaeal community structure in the sediment of eutrophic Lake Dagow: effect of temperature, Microb. Ecol., 48, 389–399, doi:10.1007/s00248-003-2027-2, 2004.
Høj, L., Olsen, R. A., and Torsvik, V. L.: Effects of temperature on the diversity and community structure of known methanogenic groups and other archaea in high Arctic peat, ISME J., 2, 37–48, doi:10.1038/ismej.2007.84, 2008.
Hung, C.-C., Tseng, C.-W., Gong, G.-C., Chen, K.-S., Chen, M.-H., and Hsu, S.-C.: Fluxes of particulate organic carbon in the East China Sea in summer, Biogeosciences, 10, 6469–6484, doi:10.5194/bg-10-6469-2013, 2013.
IPCC: Climate Change 2013: the Physical Science Basis. Contribution of Working Group I to the Fifth Assessment Report of the Intergovernmental Panel on Climate Change, edited by: Stocker, T. F., Qin, D., Plattner, G. K., Tignor, M., Allen, S. K., Boschung, J., Nauels, A. Xia, Y. Bex, V., and Midgley, P. M., Cambridge University Press, Cambridge, UK, New York, NY, USA, 1535 pp., 2013.
Jayakumar, D. A., Naqvi, S. W. A., Narvekar, P. V., and George, M. D.: Methane in coastal and offshore waters of the Arabian Sea, Mar. Chem., 74, 1–13, doi:10.1016/S0304-4203(00)00089-X, 2001.
Kao, S. J., Lin, F. J., and Liu, K. K.: Organic carbon and nitrogen contents and their isotopic compositions in surficial sediments from the East China Sea shelf and the southern Okinawa Trough, Deep-Sea Res. Pt. II, 50, 1203–1217, doi:10.1016/S0967-0645(03)00018-3, 2003.

BGD
12, 7017–7053, 2015

Karl, D. M. and Tilbrook, B. D.: Production and transport of methane in oceanic particulate organic matters, Nature, 368, 732–734, 1994.

Karl, D. M., Beversdorf, L., Björkman, K. M., Church, M. J., Martinez, A., and Delong, E. F.: Aerobic production of methane in the sea, Nat. Geosci., 1, 473–478, doi:10.1038/ngeo234, 2008.

Liikanen, A. N. U., Murtoniemi, T., Tanskanen, H., Väisänen, T., and Martikainen, P. J.: Effects of temperature and oxygenavailability on greenhouse gas and nutrient dynamics in sediment of a eutrophic mid-boreal lake, Biogeochemistry, 59, 269–286, doi:10.1023/A:1016015526712, 2002.

Li, F. Q. and Su, Y. S.: Analysis of Sea Water Masses, Qingdao Ocean University Press, Qingdao, China, 379 pp., 2000 (in Chinese).

Lin, S., Hsieh, I. J., Huang, K. M., and Wang, C. H.: Influence of the Yangtze River and grain size on the spatial variations of heavy metals and organic carbon in the East China Sea continental shelf sediments, Chem. Geol., 182, 377–394, doi:10.1016/S0009-2541(01)00331-X, 2002.

Metje, M. and Frenzel, P.: Effect of temperature on anaerobic ethanol oxidation and methanogenesis in acidic peat from a northern wetland, Appl. Environ. Microb., 71, 8191–8200, doi:10.1128/AEM.71.12.8191-8200.2005, 2005.

Middelburg, J. J., Nieuwenhuize, J., Iversen, N., Høgh, N., De Wilde, H., Helder, W., Seifert, R., and Christof, O.: Methane distribution in European tidal estuaries, Biogeochemistry, 59, 95–119, doi:10.1023/A:1015515130419, 2002.

Naqvi, S. W. A., Bange, H. W., Farías, L., Monteiro, P. M. S., Scranton, M. I., and Zhang, J.: Marine hypoxia/anoxia as a source of CH_4 and N_2O, Biogeosciences, 7, 2159–2190, doi:10.5194/bg-7-2159-2010, 2010.

Nightingale, P. D., Malin, G., Law, C. S., Watson, A. J., Liss, P. S., Liddicoat, M. I., Boutin, J., and Upstill-Goddard, R. C.: In situ evaluation of air–sea gas exchange parameterizations using novel conservative and volatile tracers, Global Biogeochem. Cy., 14, 373–387, doi:10.1029/1999GB900091, 2000.

Oudot, C., Jean-Baptiste, P., Fourré, E., Mormiche, C., Guevel, M., Ternon, J. F., and Le Corre, P.: Transatlantic equatorial distribution of nitrous oxide and methane, Deep-Sea Res. Pt. I, 49, 1175–1193, doi:10.1016/S0967-0637(02)00019-5, 2002.

BGD
12, 7017–7053, 2015

Qi, J., Yin, B., Zhang, Q., Yang, D., and Xu, Z.: Analysis of seasonal variation of water masses in East China Sea, Chin. J. Oceanol. Limn., 32, 958–971, doi:10.1007/s00343-014-3269-1, 2014.
Quay, P., Stutsman, J., Wilbur, D., Snover, A., Dlugokencky, E., and Brown, T.: The isotopic composition of atmospheric methane, Global Biogeochem. Cy., 13, 445–461, doi:10.1029/1998GB900006, 1999.
Reeburgh, W. S.: Oceanic methane biogeochemistry, Chem. Rev., 107, 486–513, doi:10.1021/cr050362v, 2007.
Scranton, M. I. and Brewer, P. G., Occurrence of methane in the near-surface waters of the western subtropical North-Atlantic, Deep-Sea Res., 24, 127–138, doi:10.1016/0146-6291(77)90548-3, 1977.
Shakhova, N., Semiletov, I., Salyuk, A., Yusupov, V., Kosmach, D., and Gustafsson, Ö.: Extensive methane venting to the atmosphere from sediments of the East Siberian Arctic Shelf, Science, 327, 1246–1250, doi:10.1126/science.1182221, 2010.
Shen, Z.: A new method for the estimation of fine-sediment resuspension ratios in estuaries – taking the turbidity maximum zone of the Changjiang (Yangtze) estuary as an example, Chin. J. Oceanol. Limn., 30, 791–795, doi:10.1007/s00343-012-2004-z, 2012.
Su, J.: Circulation dynamics of the China Seas north of 18° N, in: The Sea, vol. 11, edited by: Robinson, A. R. and Brink, K. H., John Wiley & Sons, New York, 483–505, 1998.
Tsurushima, N., Watanabe, S., and Tsunogai, S.: Methane in the East China Sea water, J. Oceanogr., 52, 221–233, doi:10.1007/BF02235671, 1996.
Upstill-Goddard, R. C., Barnes, J., Frost, T., Punshon, S., and Owens, N. J.: Methane in the southern North Sea: low-salinity inputs, estuarine removal, and atmospheric flux, Global Biogeochem. Cy., 14, 1205–1217, doi:10.1029/1999GB001236, 2000.
Wang, H., Yang, Z., Wang, Y., Saito, Y., and Liu, J. P.: Reconstruction of sediment flux from the Changjiang (Yangtze River) to the sea since the 1860s, J. Hydrol., 349, 318–332, doi:10.1016/j.jhydrol.2007.11.005, 2008.
Wanninkhof, R.: Relationship between wind speed and gas exchange over the ocean, J. Geophys. Res.-Oceans, 97, 7373–7382, 1992.
Wanninkhof, R.: Relationship between wind speed and gas exchange over the ocean revisited, Limnol. Oceanogr.-Meth., 12, 351–362, doi:10.4319/lom.2014.12.351, 2014.

BGD
12, 7017–7053, 2015

Wiesenburg, D. A. and Guinasso Jr, N. L.: Equilibrium solubilities of methane, carbon monoxide, and hydrogen in water and sea water, J. Chem. Eng. Data, 24, 356–360, doi:10.1021/je60083a006, 1979.

Yvon-Durocher, G., Allen, A. P., Bastviken, D., Conrad, R., Gudasz, C., St-Pierre, A., Thanh-Duc, N., and Del Giorgio, P. A.: Methane fluxes show consistent temperature dependence across microbial to ecosystem scales, Nature, 507, 488–491, doi:10.1038/nature13164, 2014.

Yang, J., Zhang, G. L., Zheng, L. X., Zhang, F., and Zhao, J.: Seasonal variation of fluxes and distributions of dissolved methane in the North Yellow Sea, Cont. Shelf Res., 30, 187–192, doi:10.1016/j.csr.2009.10.016, 2010.

Ye, W., Zhang, G., Zhu, Z., Huang, D., Han, Y., Wang, L., and Sun, M.: Methane distribution and sea-to-air flux in the East China Sea during the summer of 2013: impact of hypoxia, Deep-Sea Res. Pt. II, doi:10.1016/j.dsr2.2015.01.008, 2015.

Zhang, G. L., Zhang, J., Kang, Y. B., and Liu, S. M.: Distributions and fluxes of methane in the East China Sea and the Yellow Sea in spring, J. Geophys. Res.-Oceans, 109, 1–10, doi:10.1029/2004JC002268, 2004.

Zhang, G. L., Zhang, J., Liu, S. M., Ren, J. L., Xu, J. and Zhang, F.: Methane in the Changjiang (Yangtze River) Estuary and its adjacent marine area: riverine input, sediment release and atmospheric fluxes, Biogeochemistry, 91, 71–84, doi:10.1007/s10533-008-9259-7, 2008a.

Zhang, G. L., Zhang, J., Ren, J. L., Li, J. B., and Liu, S. M.: Distributions and sea-to-air fluxes of methane and nitrous oxide in the North East China Sea in summer, Mar. Chem., 110, 42–55, doi:10.1016/j.marchem.2008.02.005, 2008b.

Zhang, J.: Nutrient elements in large Chinese estuaries, Cont. Shelf Res., 16, 1023–1045, doi:10.1016/0278-4343(95)00055-0, 1996.

Zhang, J., Liu, S. M., Ren, J. L., Wu, Y., and Zhang, G. L.: Nutrient gradients from the eutrophic Changjiang (Yangtze River) Estuary to the oligotrophic Kuroshio waters and re-evaluation of budgets for the East China Sea Shelf, Prog. Oceanogr., 74, 449–478, 2007.

Zindler, C., Bracher, A., Marandino, C. A., Taylor, B., Torrecilla, E., Kock, A., and Bange, H. W.: Sulphur compounds, methane, and phytoplankton: interactions along a north–south transit in the western Pacific Ocean, Biogeosciences, 10, 3297–3311, doi:10.5194/bg-10-3297-2013, 2013.

BGD
12, 7017–7053, 2015

Table 1. Characteristics of the five cruises in the East China Sea and the Yellow Sea.

Survey period	Research vessel	CTD	Station no.
13 Mar–10 Apr, 2011	Dong Fang Hong 2	Sea-Bird 911 plus	42
11 May–7 Jun 2011	Experiment 3	Sea-Bird 911 plus	54
10–30 Aug 2011	Bei Dou	Sea-Bird 917	38
16 Oct–8 Nov, 2011	Dong Fang Hong 2	Sea-Bird 911 plus	55
20 Dec 2011–7 Jan 2012	Dong Fang Hong 2	Sea-Bird 911 plus	46

BGD
12, 7017–7053, 2015

Table 2. Temperature, salinity, and CH_4 concentrations in surface and bottom waters of the Yellow Sea and East China Sea during five cruises in 2011. Numbers indicate ranges and (averages and SD).

Season	Depth	Temperature (°C)	Salinity (psu)	CH_4 (nmol L^{-1})
Mar	surface	4.32 ~ 19.03	29.79 ~ 34.60	2.39 ~ 29.67
		(10.68 ± 3.06)	(33.16 ± 1.08)	(4.47 ± 4.09)
	bottom	5.48 ~ 16.13	32.00 ~ 34.49	2.63 ~ 30.63
		(10.06 ± 2.40)	(33.26 ± 0.75)	(5.10 ± 4.97)
May	surface	16.40 ~ 26.17	30.45 ~ 34.59	1.88 ~ 26.39
		(21.57 ± 3.00)	(33.14 ± 1.40)	(6.04 ± 5.58)
	bottom	4.00 ~ 23.92	24.21 ~ 34.90	1.31 ~ 30.36
		(15.78 ± 4.62)	(33.07 ± 1.99)	(6.41 ± 5.11)
Aug	surface	21.93 ~ 28.25	22.57 ~ 33.99	3.71 ~ 33.62
		(25.91 ± 1.45)	(30.22 ± 2.72)	(8.21 ± 6.02)
	bottom	9.01 ~ 24.99	28.69 ~ 34.47	6.20 ~ 26.22
		(20.75 ± 2.98)	(33.02 ± 1.62)	(11.88 ± 4.59)
Oct	surface	17.89 ~ 26.18	28.06 ~ 34.46	2.44 ~ 13.52
		(21.91 ± 2.26)	(32.84 ± 1.47)	(5.03 ± 1.68)
	bottom	4.12 ~ 24.19	30.87 ~ 34.67	2.50 ~ 15.24
		(17.38 ± 5.43)	(33.41 ± 1.23)	(7.51 ± 2.93)
Dec	surface	7.94 ~ 23.46	29.87 ~ 34.70	3.01 ~ 6.03
		(15.23 ± 4.28)	(33.33 ± 1.22)	(4.07 ± 0.63)
	bottom	7.84 ~ 23.45	30.91 ~ 34.73	3.03 ~ 10.20
		(14.83 ± 4.08)	(33.48 ± 1.07)	(4.53 ± 1.33)

BGD
12, 7017–7053, 2015

Table 3. Surface CH_4 saturation and sea–air CH_4 fluxes in the Yellow Sea and East China Sea.

Month	Surface saturation (%)		Wind speed ($m\,s^{-1}$)	Sea–air flux ($\mu mol\,m^{-2}\,d^{-1}$)	
	Range	Average		N2000	W2014
Mar	91–1007	155 ± 138	7.8 ± 3.8	3.95 ± 7.76	4.08 ± 8.22
May	87–1049	251 ± 221	8.8 ± 4.8	14.75 ± 25.83	15.17 ± 27.36
Aug	172–1558	390 ± 280	6.1 ± 1.6	17.65 ± 21.72	16.98 ± 21.40
Oct	101–558	222 ± 68	6.6 ± 3.0	9.87 ± 9.61	9.88 ± 9.97
Dec	106–238	157 ± 29	8.3 ± 2.8	6.64 ± 6.44	6.82 ± 6.86

BGD
12, 7017–7053, 2015

Table 4. Data used for calculation of the CH_4 budget in the East China Sea.

Parameter	Summer	Winter
Water exchange between ECS and YS (Sv)	−0.009[a]	0.013[a]
Evaporation (Sv)	−0.0068[a]	−0.010[a]
Rainfall (Sv)	0.031[a]	0.0062[a]
Terrestrial input (Sv)	0.0393[a]	0.0122[a]
Taiwan Strait water (Sv)	2.39[a]	1.22[a]
Kuroshio water (Sv)	0.89[a]	1.81[a]
Outflow of ECS (Sv)	−3.33[a]	−3.05[a]
Avg. CH_4 concentration in Changjiang (nM)	87.90[b]	173.26[b]
Avg. CH_4 concentration in TWCW (nM)	6.11[c]	4.26
Avg. CH_4 concentration in Kuroshio (nM)	3.34[c]	2.91
Avg. CH_4 concentration in YS (nM)	6.56[d]	4.33
Avg. CH_4 concentration in shelf of ECS (nM)	5.44[c]	4.31
Sea–air CH_4 flux ($\mu mol\,m^{-2}\,d^{-1}$)	16.98	9.09
Avg. sediment–water CH_4 flux ($\mu mol\,m^{-2}\,d^{-1}$)	1.78	0.94

Note: Positive values represent water import from an external source and negative values represent water export from the ECS. 1 Sv = $10^6\,m^3\,s^{-1}$.
[a] Data from Zhang et al. (2007).
[b] Unpublished data from an on-going monitoring project at Xuliujing station in the lower Changjiang.
[c] Data from Ye et al. (2015).
[d] Unpublished data from observations in July 2013.

BGD
12, 7017–7053, 2015

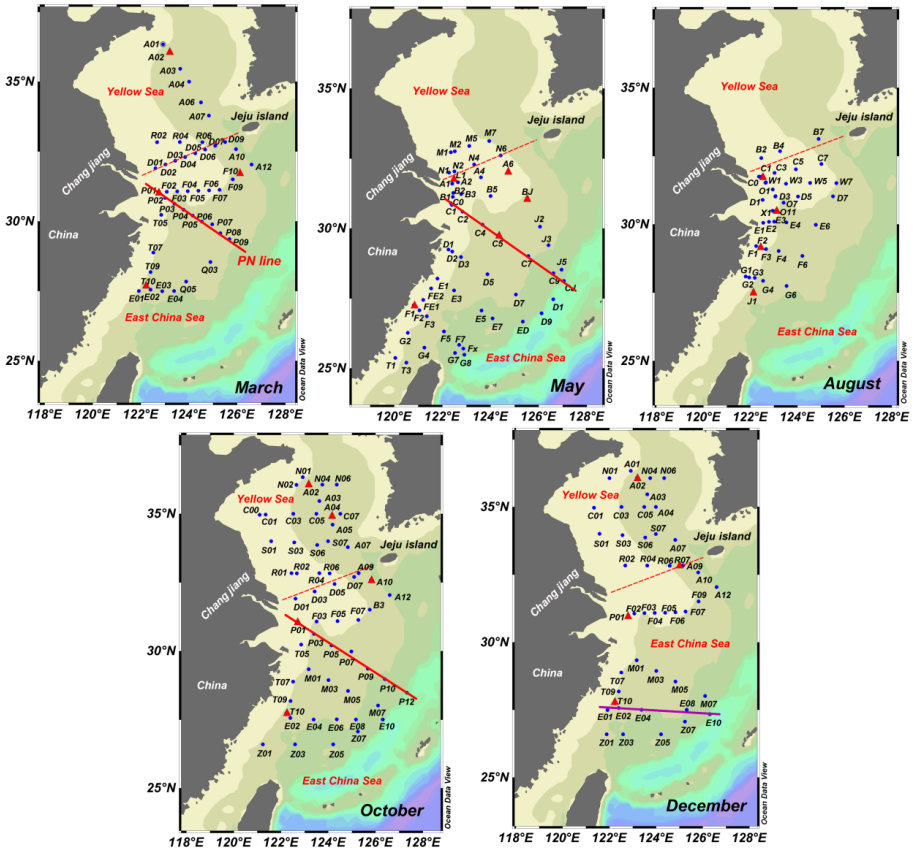

Figure 1. Sampling locations in the East China Sea and the Yellow Sea during the five cruises in 2011. Blue solid circles: seawater sampling locations; red solid triangles: sediment sampling locations; red solid line: PN line; red dashed line: boundary between the East China Sea and the Yellow Sea; purple solid line: section E.

BGD
12, 7017–7053, 2015

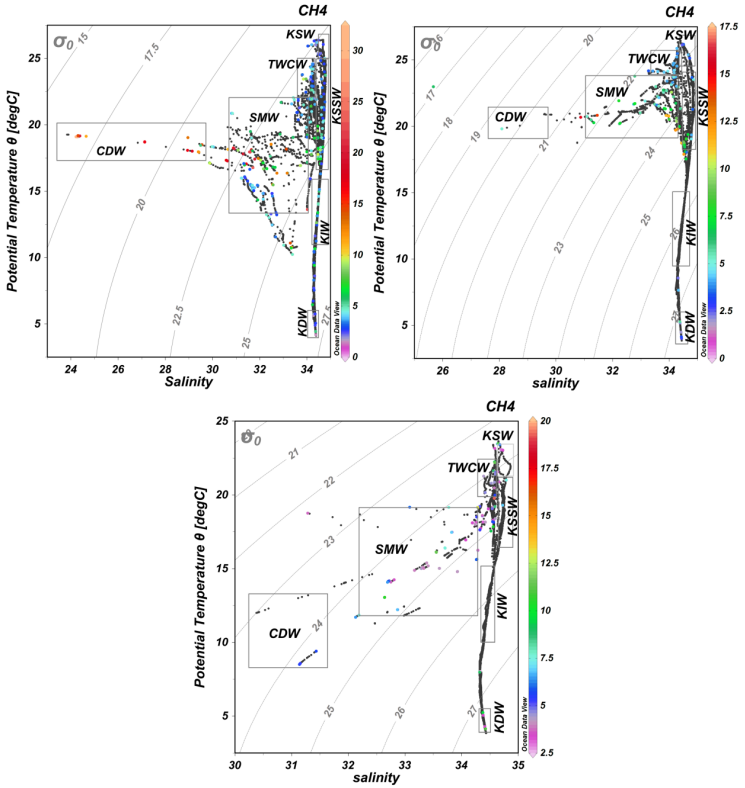

Figure 2. Temperature–salinity diagrams and CH_4 concentrations in the East China Sea during May, October, and December of 2011. The dominant water masses are classified as previously described (Li and Su, 2000; Qi et al., 2014) and indicated by rectangular outlines. CDW: Changjiang-Diluted Water; SMW: Shelf-Mixed Water; KSW: Kuroshio Surface Water; KSSW: Kuroshio Subsurface Water; KIW: Kuroshio Intermediate Water; KDW: Kuroshio Deep Water; TWCW: Taiwan Warm Current Water. Black dots: non-CH_4 sampling point; Color dots: CH_4 sampling points.

BGD
12, 7017–7053, 2015

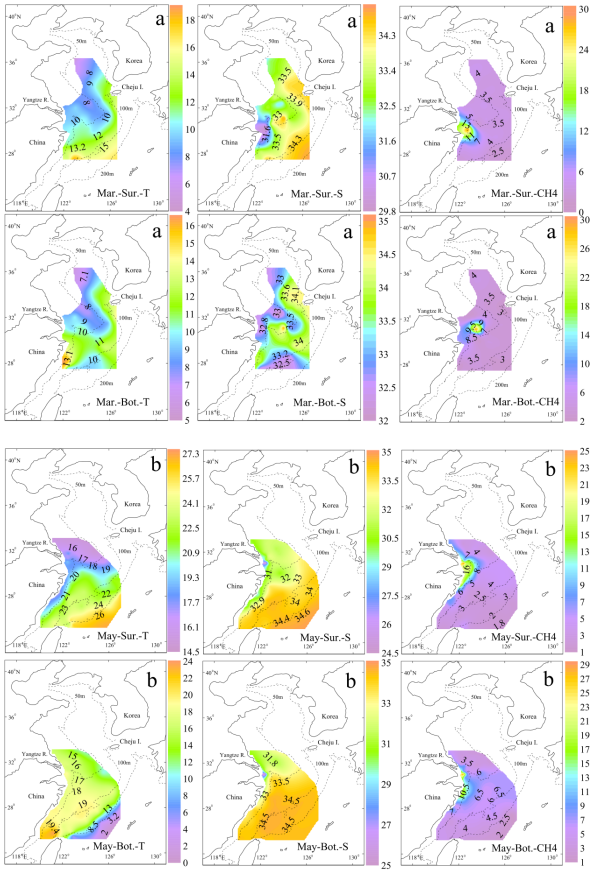

Figure 3. Geographical distribution of temperature (°C), salinity (psu), and CH_4 (nmol L^{-1}) in surface and bottom waters of the study area during March **(a)**, May **(b)**, August **(c)**, October **(d)**, and December **(e)** of 2011.

BGD
12, 7017–7053, 2015

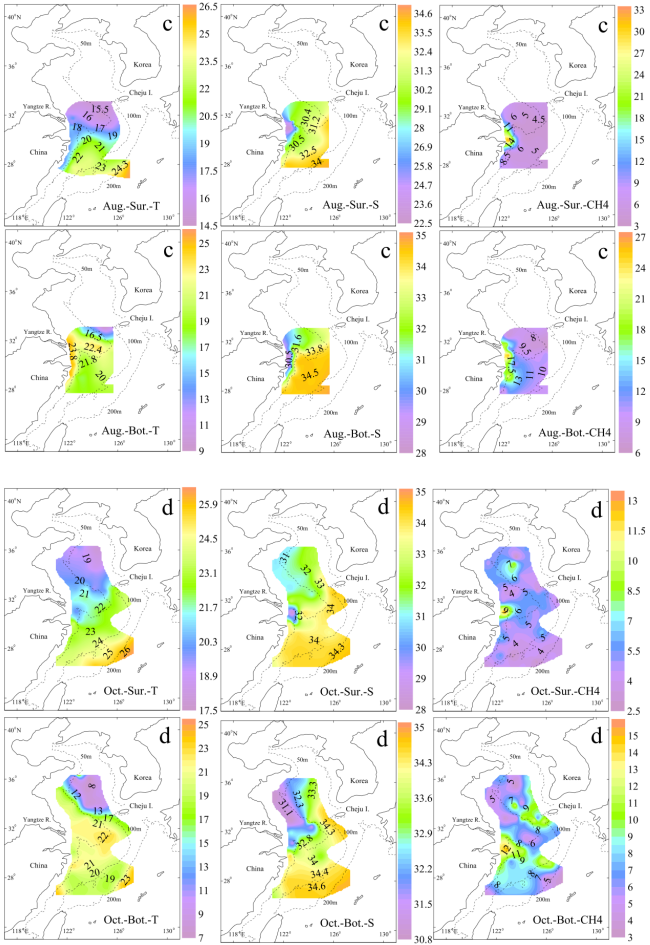

Figure 3. Continued.

BGD
12, 7017–7053, 2015

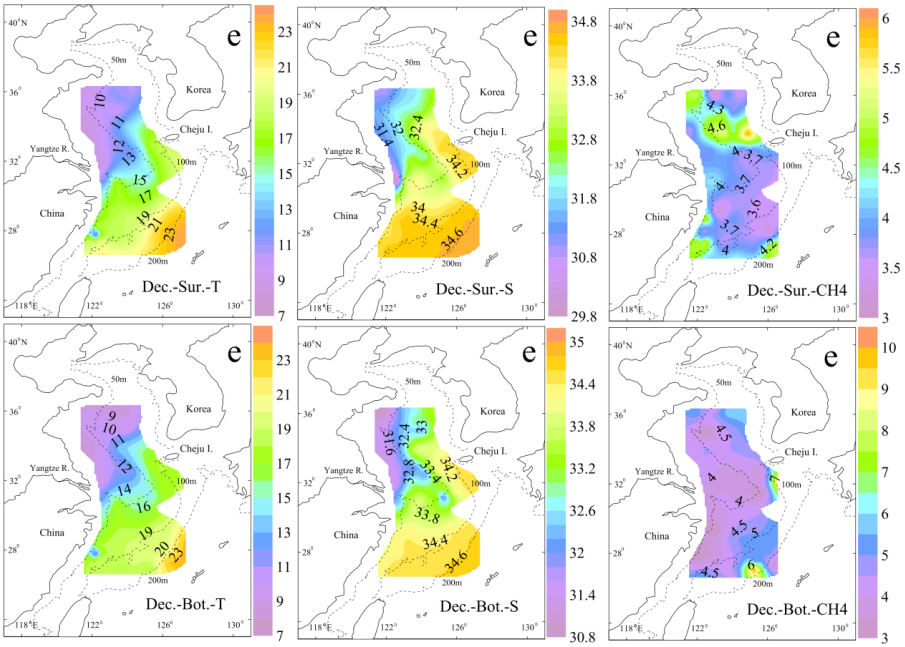

Figure 3. Continued.

BGD
12, 7017–7053, 2015

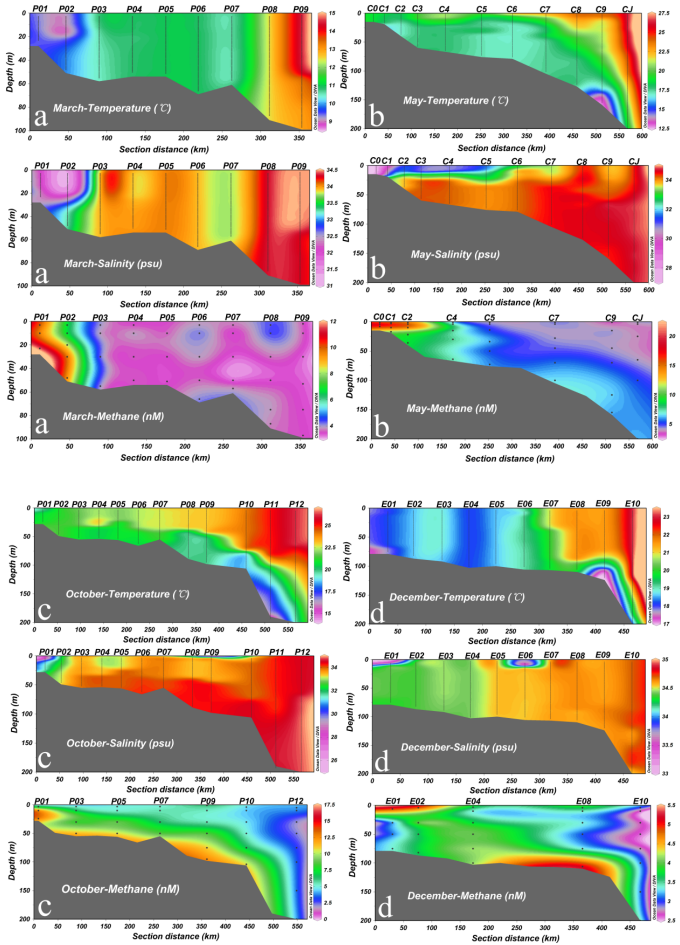

Figure 4. Depth distributions of salinity (psu), temperature (°C), and CH_4 (nmol L^{-1}) along section PN during March **(a)**, May **(b)** and October **(c)** and section E during December **(d)**.

BGD
12, 7017–7053, 2015

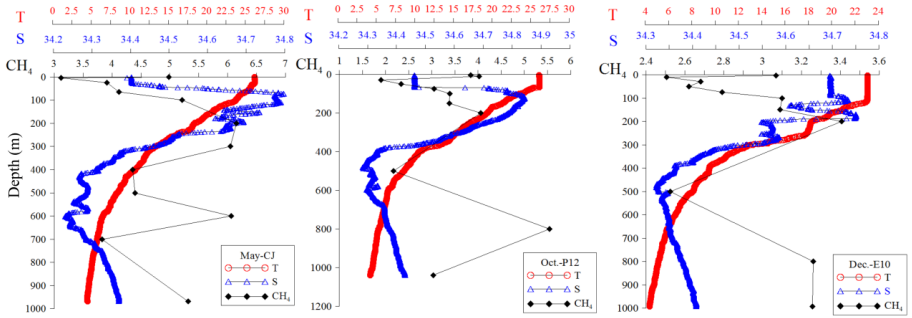

Figure 5. Depth profiles for CH_4 (nmol L^{-1}), salinity (psu), and temperature (°C) at station CJ in May, station P12 in October, and station E10 in December.

BGD
12, 7017–7053, 2015

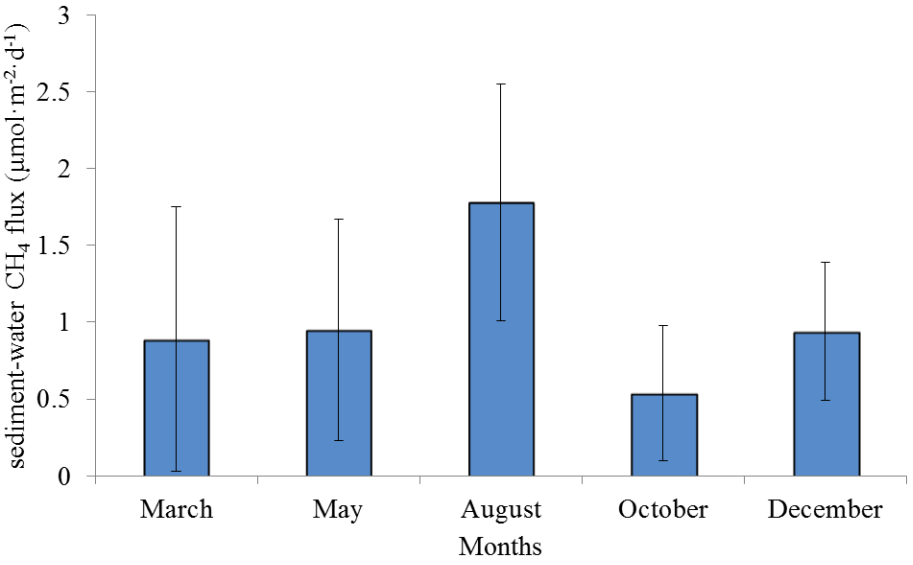

Figure 6. Seasonal variation of sediment–water CH_4 fluxes from the East China Sea and Yellow Sea.

BGD
12, 7017–7053, 2015

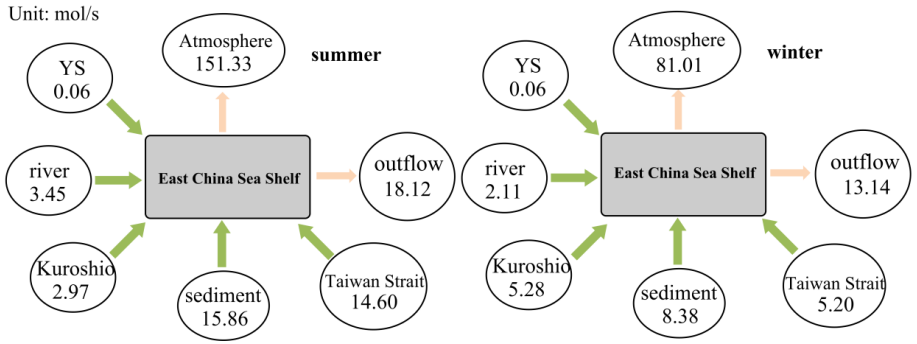

Figure 7. CH_4 budget of the East China Sea during summer and winter.

BGD
12, 7017–7053, 2015